Engineering and Technology Journal
Journal homepage: engtechjournal.org

Design of Efficient Inductive Power Link with Small Size Planar Spiral Coil Receiver for Medical Applications

Muammer M. Omran [a*], Ahmed S. Ezzulddin [b], Saad Mutashar [c]

[a] Electrical Department,University of Technology, Baghdad, Iraq. mmu_kufa@yahoo.com

[b] Electrical Department, University of Technology, Baghdad, Iraq. 30036@uotechnology.edu.iq

[c] Electrical Department,University of Technology, Baghdad, Iraq. 30099@uotechnology.edu.iq.

*Corresponding author.

Submitted: 08/05/2019 Accepted: 31/08/2019 Published: 25/02/2020

K E Y W O R D S

Biomedical devices, implantable microelectronic devices, inductive power link, printed spiral coil, WPT.

A B S T R A C T

The efficiency of a WPT system greatly depends on both the geometry and operating frequency of the transmitting and receiving structures. Genetic optimizations algorithms are presented to prepare the proposed design parameters using MATLAB to optimize the link efficiency. Single and double layer PSCs are optimally designed with minimal proximity losses effect. In this paper, we used the benefit of a double layer technique to miniaturize the receiver PCS size. The proposed single layer (10×10) mm^2 and double layer (8×8) mm^2 PSCs are validated and simulated using HFSS 15.03 software at a frequency of 13.56MHz in both cases of the air, and human biological skin tissue as intermediate material between the transmitter and receiver PSCs. The calculated and simulated results of both proposed receiver PSCs are compared for both cases of intermediate materials for their efficiency behaviors. The results show that in the case of biological tissue, the deterioration in PTE using 8mm double layer receiver is only 6.5 % (PTE =70.96%), which is less than 13.5 % (PTE=68.6%) using single layer 10mm receiver. A comparative survey has been done for similar works of different authors in the last decade. In comparison with other works, the proposed double layer (8×8) mm^2 PSCs is smaller in size and more efficient for use in the IMDs.

How to cite this article: M. M. Omran, A. S. Ezzuldin and S. Mutashar, “Design of efficient inductive power link with small size planar spiral coil receiver for medical applications,” *Engineering and Technology Journal*, Vol. 38, Part A, No. 02, pp. 199-210, 2020.

DOI: : https://doi.org/10.30684/etj.v38i2A.293

1. Introduction

The subject of inductive wireless power transmission (IPT) for powering Implantable Medical devices (IMD) is a very old matter. The first reported use of inductive power transfer (IPT) was in the 1960s that introduced IPT to transfer power to an artificial heart [1]. Then, much studies and researches are developed over the last decades to improve this type of WPT and the applications that utilizing it has been extended. The heart rate control, artificial retina, cardiac pacemakers, cochlear implants, and functional electrical stimulation [2] are examples of such applications. There are several methods for getting the energy to powering IMDs [3]. The inductive power link technique is the most widely used method for powering the IMDs. In this technique, the external coil represents the power transmitter that generates a magnetic field that cuts the implant coil turns to produce an inductive power in it, and it acts as a receiver. WPT is less efficient than using the battery, but it is more efficient than the other energy sources. WPT is a clean, safe and long-lifetime technique that converts energy from RF electromagnetic EM waves into an induced voltage. Inductive coupling wireless power transfer (WPT) used when operating distances are small, on the order of 10 mm, this is the case with many biomedical implants [4]. The external and internal coils are usually implemented using Planar Spiral Coil (PSC). A simplified block diagram of the biomedical inductively coupled telemetry system is shown in Figure 1.

The inductive link is often the weakest link in this application. Power transfer efficiency (PTE) and system miniaturization are major design specifications to evaluate a power link. Given application-related constraints, these specifications are inherently correlated, and a careful trade-off analysis is required to achieve optimal performance. Therefore, the power transmission link should be designed in a way that it achieves high PTE and provides sufficient power to the load while considering practical limitations.

This work is a continuation of the extensive investigations of previous studies to achieve the optimal efficient PTE with smaller coil size suitable and feasible for use in the IMDs applications. Table IV illustrates the literature survey and comparison between this work and some of the previous studies.

2. Mathematical Modelling of Single Layer PSC Inductor

I. Square single layer PSC inductance

Figure 2 shows an equivalent circuit diagram of the WPT system. $L1$ is typically driven by a class E amplifier, which has the benefit of high efficiency. Rs_1, Rs_2 and C_{p1}, C_{p2} are parasitic resistance and capacitance of the transmitter and receiver PSCs, respectively. $C1$ and $C2$ are the transmitter and receiver PSCs resonance tuning capacitors to make them resonate on the same frequency to achieve high voltage gain and maximum power transfer efficiency.

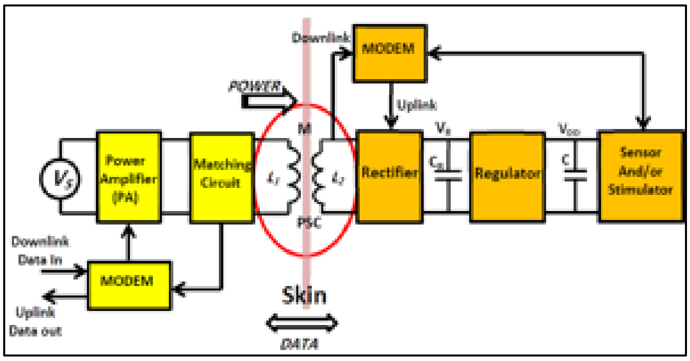

Figure 1: Block diagram of a passive biomedical inductive power link system

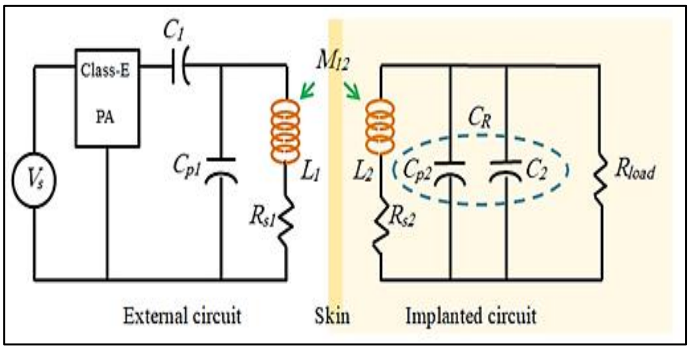

Figure 2: Simplified WPT equivalent circuit

There are several coil shapes are utilized in different WPT applications, the mutual inductance M and the quality factor Q of the coils are the most important circuit parameters that are affecting the power transfer efficiency PTE are dependent on the coil shape and geometry includes the relative distance, orientation, and the number of turns. Square spirals are popular because of the ease of their layout and generated easily even in simple layout tools [5]. To simplify the design of PSC, Figure 3 illustrates the simplified schematic diagram of a square PSC with its equivalent lumped RLC commonly used model. The planar coil has self-inductance L, series resistance Rs, and parasitic capacitance C_p. The number of turns n, line width w, line spacing s, outer diameter d_o, inner diameter d_i, are the geometric parameters of the PSCs that mainly affect the circuit parameters such as L, Q, and k, and therefore the PTE, are [6].

The self-inductance for a square-shaped PSC inductor is presented in the Eq. (1) [6].

$$L = \frac{1.27\mu n^2 d_{avg}}{2}\ [\ln(\frac{2.07}{\varphi}) + 0.18\varphi + 0.13\varphi^2] \quad (1)$$

Where $\mu = \mu_0\mu_r$ is the relative permeability, μ_0 is the permeability of free space, and μ_r is the relative permeability of the conductor. n is the number of turns, φ is the fill factor parameter can be found from (2) which changes from 0 to 1, when all the coil turns are concentrated on the perimeter, and the turns spiral directed all the way to the center of the coil [6].

$$\varphi = \frac{d_o - d_i}{d_o + d_i} \quad 0 \leq \varphi \leq 1 \quad (2)$$

The average diameter of the coil (*davg*) in Eq. (1) is given in Eq. (3):

$$d_{avg} = \frac{(d_o + d_i)}{2} \quad (3)$$

The number of turns of the PSC can be calculated by Eq. (4):

$$n = \frac{d_o}{(s+w)} \cdot \frac{\varphi}{(1+\varphi)} \quad (4)$$

From Eq. (5) below, we can calculate the inner and the outer coil diameters based on the number of turns n, s and w of the coil conductor as:

$$d_o = d_i + (2n+1)w + (2n-1)s \quad (5)$$

The smaller spacing s improves the inter-winding magnetic coupling and reduces the area consumed by the spiral. A large spacing is desired to reduce the inter-winding capacitance and parasitic losses. Therefore, ratio *s/w* must be carefully selected by the designers, because it exhibits a maximum error of 8% for $s \leq 3w$. Typically, spiral inductors are built with $s \leq w$ [7].

II. Quality factor

The quality factor of the inductor is an important parameter that has a high impact on the link power efficiency. To determine the quality factor of PSC we need to know the total impedance of the coil, which constructed from the parasitic dc resistance and parasitic capacitance. To calculate the total parasitic resistance of the PSC, we must have the length of the conductive trace *lc*, the resistivity of the conductive material ρ_c, and its thickness *tc*. Considering the skin effect δ, all the mentioned parameters can be determined using equations mentioned in [6]. The quality factor and the PSC impedance are calculated as:

$$Z = \frac{R_s + j\omega L}{1 - \omega^2 L C_p + j\omega R_s C_p} \quad (6)$$

$$Q = \frac{\omega L - \omega(R_s^2 + \omega^2 L^2) C_p}{R_s} \quad (7)$$

Where $w=2\pi f_0$, and f_0 is the operating frequency. The inductance and quality factor of individual PSC can be easily calculated from Eq. (8) and Eq. (9) respectively by using Z-parameters as the following formulas [8].

$$L = \frac{\mathrm{Im(Z)}}{2\pi f} \quad (8)$$

$$Q = \frac{\mathrm{Im(Z)}}{\mathrm{Re(Z)}} \quad (9)$$

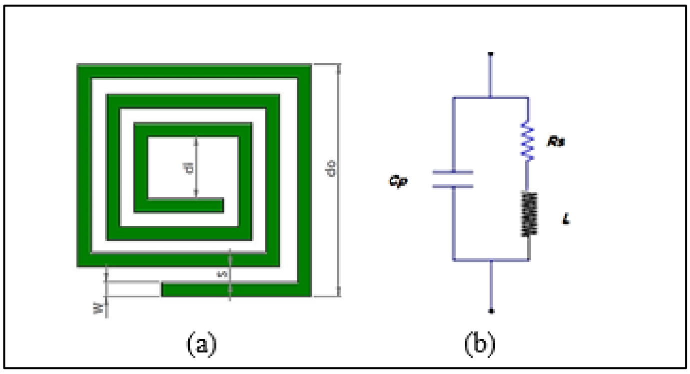

Figure 3: (a) Geometry parameters of a square planar spiral inductor .(b) Lumped RLC model of PSC

III. Mutual inductance of PSCs

The geometric shape and parameters such as the line width w_1 and w_2, the line spacing s_1 and s_2, the outer radii are d_{o1} and d_{o2}, the distance between coils d_r, and the number of turns n_1 and n_2 are the main parameters that affect the mutual inductance M between the PSCs. The overall M can be determined by summing the partial mutual inductance values between each turn of one coil and all the turns of the other coil [6]. The total M can be determined by adding all these combinations of M. For different axial distance, the equation of M between two square-shaped planar inductors can be determined as the method presented in [9, 10, 11].

IV. Power Link Efficiency of PSCs

Power link efficiency η_{link} of the WPT system can be easily obtained at the optimum load resistance RL has chosen according to Rs_2, by multiplying both of individual efficiencies of primary and secondary coils by each other [6], which yields the formula:

$$\eta_{link} = \frac{k^2 Q_1 Q_2^2}{(Q_L+Q_2)(\frac{Q_2}{Q_L}+k^2 Q_1 Q_2+1)} \tag{10}$$

The maximum achievable power transfer efficiency of the WPT system determined as [12]:

$$\eta_{max} = \frac{k^2 Q_1 Q_2}{(1+\sqrt{1+k^2 Q_1 Q_2})^2} \tag{11}$$

V. Double layer PSC inductor

Two inductors can be arranged on top of each other using two layers and connected in series to realize a large inductance per unit area, as shown in Figure 4. Double-layer coils allow achieving a high inductance, high-quality factor and then high PTE.

Both inductor layers are connected in such a way so that the current flow through both PSCs are in the same direction, and the magnetic flux lines are in the same direction and aiding each other to produce higher mutual inductance. Therefore, the total Inductance of double-layer PSCs shown in Figure 4(a) is:

$$L_d = L_{s1} + L_{s2} + 2M_s \tag{12}$$

All the double-layer circuit parameters such as parasitic resistance and parasitic capacitance can be calculated using the expressions mentioned in [13].

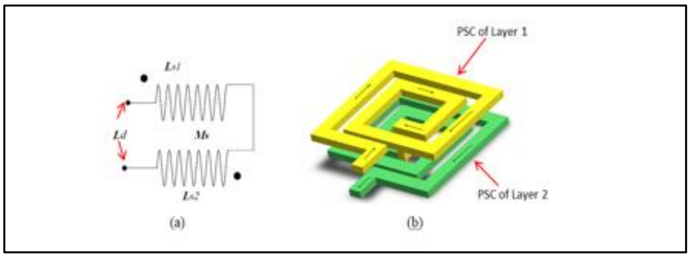

Figure 4: Geometrical parameters of a double layer PSC

VI. Square PSC design procedure

In this section, an iterative design procedure which starts with a design constraints and initial values that will be applied to the closed-form expressions that mentioned above, using MATLAB software to find the optimal transmission efficiency of the WPT link by sweeping all parameters included in the expressions [13] and observing the change in the power link efficiency η_{link}, the procedure ends with the optimal PSC pair geometries. The results and values suggested by theoretical calculations will be verified using HFSS 15.03 Electromagnetic field solver simulator. There are two types of receiver PSCs of the WPT system that has been proposed to miniaturize the receiver size and for PTE comparison purposes, single layer (10×10) mm^2, and double-layer (8×8) mm^2. The air is assumed the dielectric medium between PSCs in our calculations and software simulations. Then, the biological human tissues will be considered as the dielectric medium. The human biological tissue that was used in biomedical implanted devices applications is less than 10mm of depth. In general, the depth used for implanted microsystem stimulators is 1–4 mm, depth for retinal implants it is 5mm and the depth for cochlear implants is about 3~6mm, [14,15]. In this work, the tissue thickness is assumed to be 3mm (skin, and fat), which will be enough as a simulation depth of implanted PSC.

1) Applying the design constraints: Wireless link efficiency is affected by a set of parameters such as coils Q-factor and coupling coefficient k, *which* is limited by other factors related to the application and fabrication of technical considerations of the implantable device. The priority is to define the overall size constraints depending on where the implant will be located inside the body to indicates the minimum size features that result in acceptable yield in manufacturing. Table 1 shows the initial values and design constraints imposed by the application and fabrication technology. The typical size of the implanted coil has been used is (10×10) mm^2. The coupling distance between the PSCs is considered (D=10) mm. The operating frequency is chosen to be 13.56 MHz, which has been, designated an ISM band by the international ITU, and it is compatible with Radio Frequency Identification (RFID) standards [16,4]. The magnetic field strength H for a coil with a turn's number of n and radius d_o along the axial distance (D) from the center of the coil can be given from [17] as:

$$\mathrm{H} = \frac{\mathrm{I.n.}d_o^2}{2\sqrt{(d_o^2+D^2)^3}} \tag{13}$$

To find the mathematical relationship between the maximum field strength H and the coil radius d_o by differentiating H in Eq. (14) to d_o and solving for the roots:

$$d_o = D.2\sqrt{2} \tag{14}$$

From this expression, we can estimate the external coil size as (28×28) mm^2, where D=10mm from the Table 1. Figure 5 shows the coupling coefficient versus variable values of external PSCs outer and inner diameters while the implanted PSC outer diameter fixed as 10mm with a distance between them of D=10mm. It is clear that a good choice for d_{o1}value that maximizes k would be d_{o1}=28mm, d_{o2}=10mm, The optimal d_{i1} and d_{i2} that maximize the coupling coefficient k can be found by fixing d_{o1}= 28mm, d_{o2} =10mm, then calculate the mutual inductance and coupling coefficient for different values of d_{i1} and d_{i2} by sweeping them around a wide range of initial values. Figure 6 shows the optimal d_{i1} between 5 to 6 mm. the chosen values for d_{i1}= 5.5 mm, and d_{i2}= 5 mm to obtain a higher value of coupling coefficient k. The initial values selected for the conductive line spacing and the line width are set to their minimum values (s_1= s_2= 0.15mm, and w_1= w_2= 0.15 mm).

Table 1: Design constraints and initial values

Parameters		Symbol	Design Value
Design Constraints	Operating frequency	f_o	13.56MHz
	Implanted coil outer diameter	d_{o2}	≤ 10mm
	The relative distance between coils	D	10mm
	Secondary loading resistance	R_L	100-500 Ω
	Minimum conductor spacing	$s_{\min}$	0.15mm
	Conductor thickness	t_c	≤ 0.07mm
	The resistivity of material*	ρ	16.8 nΩm
	Substrate thickness	t_s	≤ 1mm
	Substrate dielectric constant	ϵ_{rFR4}	4.4
Initial Values	Receiver inner diameter	d_{i2}	5mm
	Transmitter and Receiver conductor spacing	s_1, s_2	0.15mm
	Transmitter and receiver conductor width	w_1, w_2	0.15mm

*Copper

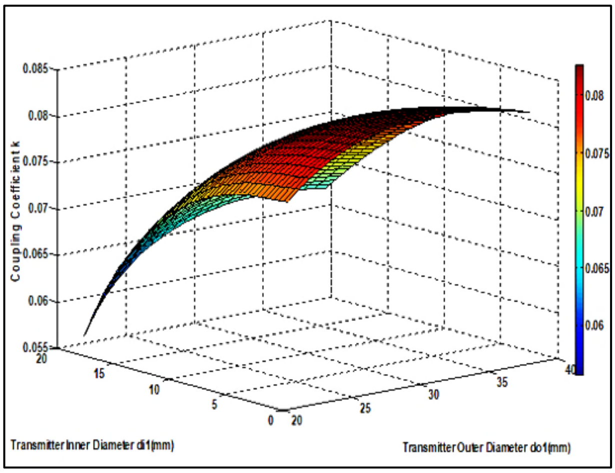

Figure 5: Optimizing of di1, do1 with respect to k where initial values of do2 and di2 are 10mm and 5mm respectively

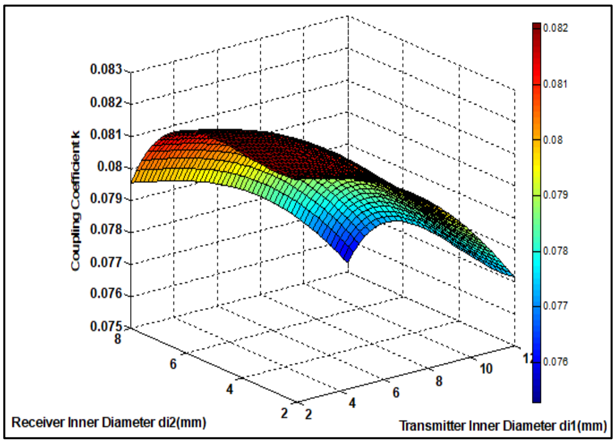

Figure 6: Optimizing of di1, di2 with respect to k. at a distance between coils of 10mm

1) Optimizing line width and coil turns of Transmitter PSC: By plugging the coil parameters initial values defined in the previous step into expressions mentioned in section (2. math.modelling) in two consecutive stages. In the first stage of this step, the quality factor Q_1, and the power link efficiency η_{12} are calculated for different values of w_1, s_1 which swept in a wide range above their initial values. The transmitter PSC number of turns n_1 is determined by using Eq. (1) to Eq. (4) using the optimal values of w_1, and s_1. The fill factor for the transmitter PSC is found to be φ_1=0.67 using Eq. (2). Since w_2, s_2 is kept constant for this step, modifying w_1 directly affects k, Q_1, and η_{12}. However, the parasitic capacitance and proximity effects must be considered, and the coil self-resonant frequency must be higher than operating frequency [18]. However, it is known that proximity effect losses increase with increasing metal width (w) [19]. For this stage, the higher value of Q_1, and η_{12}, and the optimal line width w_1 and line spacing s_1 are recorded for further optimization in the next stage. In the second stage of this step, the quality factor Q_1, and power link efficiency η_{12} are recalculated once again for the new optimal value of Q_2 which obtained after the receiver PSC parameters optimization. Finally, to reduce proximity effect losses, and parasitic losses, the line spacing (s) must be increased. All the obtained results of the transmitter PSC parameters are listed in Table 3.

2) Optimizing line width and coil turns of receiver PSC: In this step, the receiver coil size of (10×10) mm^2 is chosen. Using the parameter values issued from previous steps such as d_{o2}, and d_{i2}, the fill factor value would be (φ_2= 0.33). Again, as the optimization of the transmitter, PSC is implemented, the quality factor Q_2 for the receiver PSC is calculated while sweeping w_2, and s_2 around its initial values ($s_{2\min}$, $w_{2\min}$ = 0.15 mm). The corresponding optimal number of turns n_2 of the receiver PSC calculated with respect to the maximum link efficiency using different values of load resistance RL would be n_2=5 turns at η_{link} = 83% as shown in Figure 7. It is clear from this figure that the optimal load resistance for this case is 100 Ω. Table 3 shows the final values of the design optimization process.

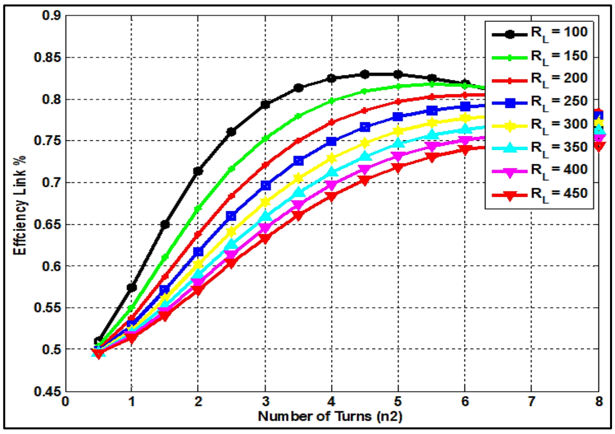

Figure 7: Optimizing the number of turns of the PSC receiver using different load resistance values in (Ohm)

All the design steps for PSC parameters optimization are shown in Figure 8.

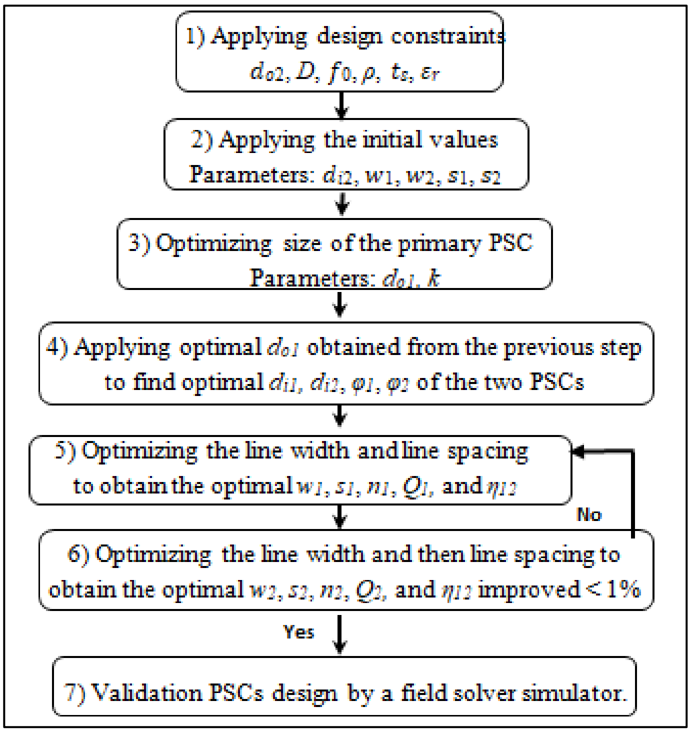

Fig.8: Optimization PSCs design procedure flowchart

VII.PSC Modeling in HFSS EM Simulator

1) Transmitter and Single Layer (10×10) mm^2 PSC Receiver:

The PSCs geometry parameters obtained after optimization processes can be modelled and verified using HFSS 15.03 solver simulator software. Figure 9 shows both transmitter and receiver PSCs modelled with the air as insulation media between coils, and the substrate material is FR4. The simulation process implemented by sweeping the PSCs model around the operating frequency f_o=13.56MHz at a fixed distance between PSCs (D=10mm) to find the Z-Parameters for both PSCs at the operating frequency. The output variables of the simulation process like inductance L, quality factor Q, mutual inductance M, and the coupling coefficient k of the modelled system can be determined using the Z parameters equations in [10].

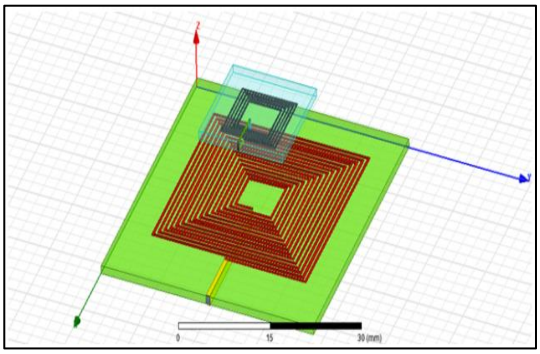

Figure 9: Transmitter and receiver PSCs modelled in HFSS 15.03

The final geometries and parameters result of the applied WPT link are defined in Table 3.

2) Transmitter and Double Layer (8×8) mm^2 PSC Receiver:

A double layer (8×8) mm^2 square-shaped PSC receiver is proposed. The proposed approach maximizes the use of the surface area by miniaturizes the PSC size to provides approximately the same high efficiency and robustness performances as larger size single layer PSC. In the double-layer PSC technique, the conductor width *w* and the line spacing s can be increased in such a way that reduces the series resistance and increases the quality factor of PSC with the considerations of proximity and parasitic losses. The Optimization procedure of the double layer PSC is the same as that of single-layer PSC mentioned in previous sections. The resulting parameters of the PSC's geometries after the optimization processes are shown in Table 3.

Figure 10 shows the transmitter and double layer receiver PSCs model built with HFSS 15.03 simulator software. The simulation results indicate that despite the small size of the double layer receiver PSC, the obtained efficiency of a double layer (77.4 %) is decreased only by 5% whereas the receiver size is decreased by 20% compared to that of single-layer (10×10) mm^2. The maximum Power link efficiency is shown in Figure 11. All of the calculated and simulated results of the single- and double-layer PSCs are compared in Table 3. Figure 12 illustrates that the optimal load resistance for simulated double-layer PSC is 300 Ohm.

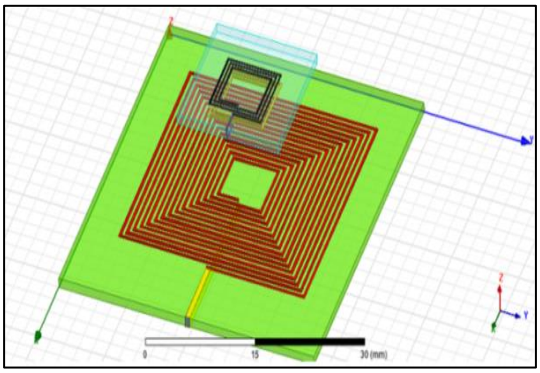

Fig. 10: Transmitter and double layer receiver PSCs modelled in HFSS 15.03

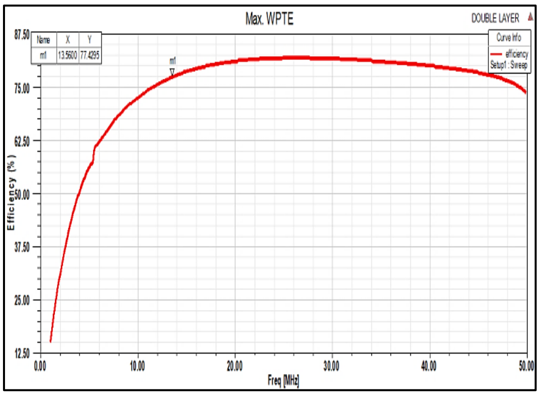

Figure 11: Power Transmission Efficiency of the double layer PSCs

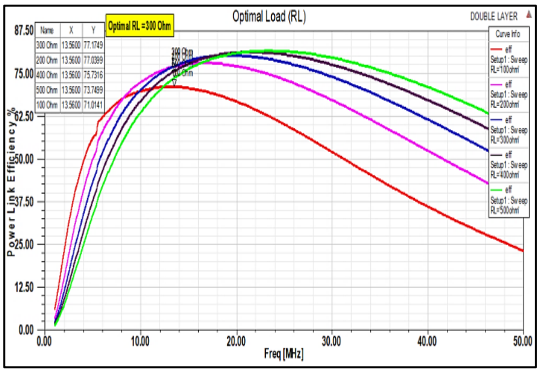

Figure 12: Power link efficiency with different load resistances at and 10 mm transmission distance

3) EM Simulation with Human Skin Tissue:

The PSCs are designed for power transmission across biological tissue as the medium between the transmitter and receiver PSC pairs. These human tissues have frequency-dependent dielectric properties. Table 2 shows the dielectric properties of human tissue materials [15]. Because the transcutaneous implanting process is implemented between muscle and fat layers, therefore, only two layers that represent the main human skin tissue layers have been used which is reasonable for nerves and muscle stimulation applications. The distance between transmitter and receiver PSCs would be 3mm divided as a 1mm wet-skin layer followed by 2mm fat layer. Figure 13 illustrates the modelling of transmitter and receiver PSCs in the HFSS software simulator with the human skin tissue as a biological intermediate material.

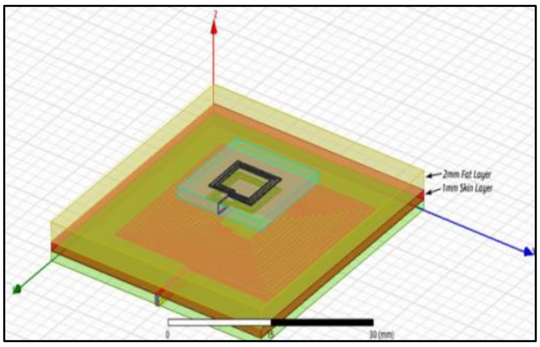

Figure 13: HFSS 15.03 EM field solver simulator modelling of double-layer (8x8) mm2 PSCs receiver with human biological tissue

Table 2: Electrical properties of Human biological tissue at the range of 13.56MHz [15]

Tissue material	Conductivity (s/m)	Relative Permittivity	Loss Tangent
Wet Skin	0.3842	177.13	2.8754
Fat	0.030354	11.827	3.4021

3. Simulation Results and Discussion

The simulation results indicate that the maximum power transfer efficiency is degraded for both single layer and double layer receiver PSCs in the case of the existence of the tissue. The maximum power transfer efficiency for the single and double layer are decreased to 68.6% and 70.96% respectively, in the case when tissue exists between the two coils as it is clear from Figure 14. The Near-field radiation patterns for the simulated WPT transmitter and double layer receiver PSCs with the human biological tissue as intermediate material is shown in Figure 15, the total electric near-field of E-total around the PSCs reactive region in the range of both azimuth and elevation angles is shown in dB. The result shows that the maximum E-total is -70.7113dB.

Table 3: The results of geometry parameters optimization based on both the calculations and simulations processes

Parameter	Transmitter PSC TX1	TX2	Single Layer RX1	Double Layer RX2
d_o(mm)	28	28	10	8
d_i(mm)	5.5	5.5	5	5.1
n (turn)	15	15	5	3$_{\text{(each layer)}}$
W(mm)	0.34	0.32	0.22	0.2
s(mm)	0.41	0.43	0.28	0.3
L(μH)	3.97	4.0258	0.2707	0.2944
Q_{simu}	178.23	171.98	84	78.47
K_{calc}	0.0815 single 0.0658 double			
$K_{simu}{}^{\Diamond}$	0.0828 single 0.0671 double			
$\eta_{calc}{}^{\dagger}$.	83.5% single 79.4% double			
$\eta_{simu}{}^{\Diamond}$.	82.117% single 77.429% double			
$\eta_{simu}{}^{\#}$.	68.6% single 70.96% double			

† calculated for 10mm air gap, ◊simulated with 10mm air gap, # simulated with 3~4mm biological tissue.

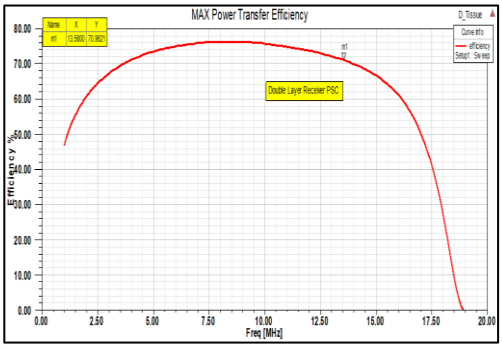

Figure 14: PTE of double-layer PSC system with human tissue

A comparative analysis has been done to compare this work with other various techniques proposed by different authors throughout the last decade. The comparison clarifies the contribution of this work to the WPT technique as illustrated in Table 4. It can be observed from the comparison that this work provides the smaller PSC size and efficient inductive power link than other proposed works which will reflect on the performance of IMD and from the other side on the patients who utilize implanted sensors or medical devices and give them more flexibility in their lifestyle which represents the significance of this work.

Table 4: Comparison with the results of other previously published works.

References	Year	Technique	PSC Shape	Operating Freq. MHz	Medium	Tx Size (mm) d_o	d_i	Rx Size (mm) d_o	d_i	Efficiency % *Calculation*	*Simulation*
[5]	2009	2 coils	square	13.56	Air	38	14.9	10	5.8	72.05	74.86
					saline	30	11.1	10	5.5	55.22	49.12
					muscle	24	9.4	10	7.2	29.58	27.70
[7]	2011	2 coils	square	13.56	Air	28	8	10	6	77.5	71.1
				8	Skin+Fat					-	15.2
[19]	2015	2 coils	Circular	13.56	Skin+Fat	30	-	10	4.3	-	55
											60
[8]	2017	2-coils 1~2Layers	square	13.56	Air	32	6.1	12	5	79.99	80.74
[20]	2018	2-coils 1~3Layers vari-width	square	13.56	Air	80	10	23	3.4 11.4	-	-
This work	2019	2- coil 1~2Layers	square	13.56	Air	28	5.5	8	5.1	79.4	77.4
					Skin+Fat					-	70.96*

*At distance = 3mm in biological skin tissue simulation.

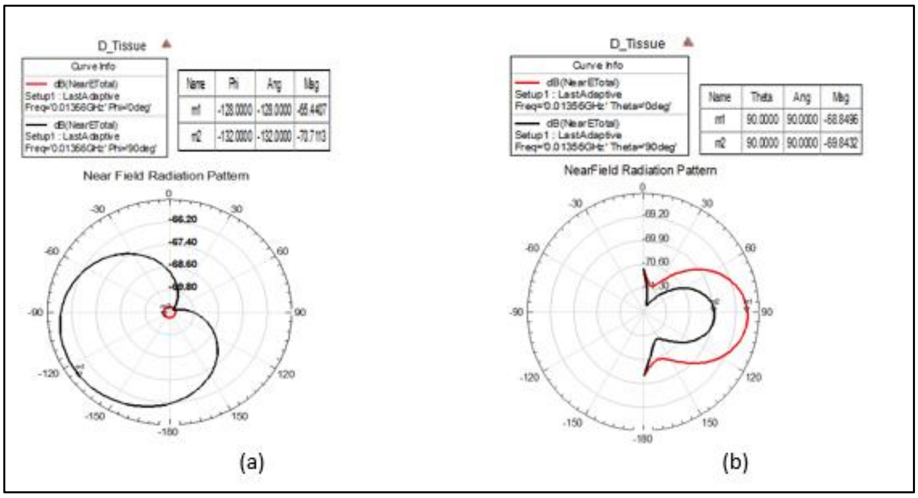

Figure 15: Simulated radiation patterns for WPT transmitter and double layer receiver PSCs with the human biological skin tissue as intermediate material with (a) The azimuthal plane (θ = 0◦, and 90◦), and (b) The elevation plane (φ= 0◦, and 90◦), respectively

4. Conclusions

The results indicate that the losses through biological tissue media are lower at low frequencies (about 7.5MHz). The presence of the biological tissue decreases the self-resonance-frequency (SRF) of the PSCs. As it is clear from the results, in spite of its small size, the maximum PTE of the double layer (8×8) mm^2 receiver is decreased only by 6.4% less than the case of air gap, whereas the maximum PTE of the single-layer (10×10) mm^2 receiver is decreased by 13.5% even when both PSCs are in the same environments. According to these results, the proposed small size double layer (8×8) mm^2 is more efficient and feasible to use in IMD applications than the larger size single layer PSC of (10×10) mm^2.

References

[1] C. Chestek, V. Gilja, P. Nuyujukian, R. Kier, F. Solzbacher, S. Ryu, R. Harrison, S. K. Hermes, “Low-power wireless neural recording system for freely moving primates,” IEEE Trans. Neural Syst. Rehabil. Eng., 17, 4, 330–338, 2009.

[2] A. Kiourti, K. S. Nikita, “Design of implant antennas for medical telemetry: Dependence upon operation frequency, tissue anatomy, and implantation site,” Int. J. Monit. Surveillance Technol. Res., 1, 1, 16–33, 2013.

[3] M. A. Hannan, S. Mutashar, S. A. Samad, A. Hussain, “Energy harvesting for the implantable biomedical devices: issues and challenges,” Biomed Eng. Online. DOI: 10.1186/1475-925X-13-79. Review. 2014.

[4] U. Jow and M. Ghovanloo, “Design and optimization of printed spiral coils for efficient transcutaneous inductive power transmission,” IEEE Transactions on biomedical circuits and systems, Vol. 1, No. 3, pp. 193– 202, Sep. 2007.

[5] S. S. Mohan, M. Hershenson, S. P. Boyd, and T. H. Lee, “Simple accurate expressions for planar spiral inductances,” IEEE Journal of Solid-State Circuits, Vol. 34, No. 10, October 1999.

[6] U. Jow and M. Ghovanloo, “Design and optimization of printed spiral coils for efficient transcutaneous inductive power transmission,” IEEE Transactions on biomedical circuits and systems, Vol. 1, No. 3, pp. 193– 202, Sep. 2007.

[7] C. P. Yue, C. Ryu, J. Lau, T. H. Lee, and S. S. Wong, “A physical model for planar spiral inductors on silicon,” in Proc. IEEE Int. Electronic Devices Meeting, San Francisco, CA, 1996.

[8] W. Wu and Q. Fang, “Design and simulation of printed spiral coil used in wireless power transmission systems for implant medical devices,” Engineering in Medicine and Biology Society (EMBC) Annual International Conference of the IEEE, pp. 4018-4021, 2011.

[9] A. S. Ezzulddin and A. A. Ibraheem, “Design and optimization of printed spiral coils used in wireless power transmission systems for powering 10 mm^2 receiver size at 13.56 MHz operating frequency,” International Journal of Current Engineering and Technology, Vol.7, No. 5, 2017.

[10] S. Mutashar, M. Hannan, S. Samad, and A. Hussain, “Inductive coupling links for lowest misalignment effects in transcutaneous implanted devices,” Biomed Tech., 59, 3, 257–268, 2014.

[11] S. Raju, C. C. Parawoto, M. Chan, and C. P. Yue, "Modeling of on-chip wireless power transmission system," IEEE International Wireless Symposium (IWS), 2015.

[12] J. Olivo, S. Carrara, and G. De Micheli, "A study of multi-layer spiral inductors for remote powering of implantable sensors," IEEE transactions on biomedical circuits and systems, vol. 7, no. 4, 2013.

[13] E. Ashoori, F. Asgarian, A. M. Sodagar, and E. Yoon, "Design of double-layer printed spiral coils for wirelessly-powered biomedical implants," 2011 Annual International Conference of the Engineering in Medicine and Biology Society (EMBC), IEEE, 2011.

[14] S. Mutashar, M. Hannan, S. Samad, and A. Hussain, "Analysis and optimization of spiral circular inductive coupling link for bio-implanted applications on air and within human tissue," Sensors, vol. 14, no. 7, pp. 11522–11541, 2014.

[15] S. Mutashar, M. A. Hannan, S. A. Samad, and A. Hussain, "Design of spiral circular coils in wet and dry tissue for bio-implanted microsystem applications," Progress in Electromagnetics Research M 32, pp.181-200, 2013.

[16] K. Finkenzeller, "Fundamentals and Applications in contactless smart cards, radio frequency identification, and near-field communication," [RFID Handbuch. English], ISBN 978-0-470-69506-7 (cloth).

[17] K. Finkenzeller, "RFID handbook: fundamentals and applications in contactless smart cards and identification," 2nd ed. Hoboken, NJ: Wiley, ISBN: 0-470-84402-7, 2003.

[18] J. Olivo, S. Carrara, and G. De Micheli, "Modeling of printed spiral inductors for remote powering of implantable biosensors," Presented at the 5th Int. Symp. Med. Inf. Commun. Technol., Mar. 2011, pp. 29-32.

[19] W. B. Kuhn and N. M. Ibrahim, "Analysis of current crowding effect in multi-turn spiral inductors," IEEE Transactions on Microwave Theory and Techniques, vol. 49, no. 1, pp. 31–38, 2001.